Relaxation of synchronization on complex networks

Seung-Woo Son,[1,*] Hawoong Jeong,[1,†] and Hyunsuk Hong[2,‡]
[1]*Department of Physics, Institute for the BioCentury, Korea Advanced Institute of Science and Technology, Daejeon 305-701, Korea*
[2]*Department of Physics, Research Institute of Physics and Chemistry, Chonbuk National University, Jeonju 561-756, Korea*
(Received 10 September 2007; revised manuscript received 8 January 2008; published 14 July 2008)

We study collective synchronization in a large number of coupled oscillators on various complex networks. In particular, we focus on the relaxation dynamics of the synchronization, which is important from the viewpoint of information transfer or the dynamics of system recovery from a perturbation. We measure the relaxation time τ that is required to establish global synchronization by varying the structural properties of the networks. It is found that the relaxation time in a strong-coupling regime ($K>K_c$) logarithmically increases with network size N, which is attributed to the initial random phase fluctuation given by $\mathcal{O}(N^{-1/2})$. After elimination of the initial-phase fluctuation, the relaxation time is found to be independent of the system size; this implies that the local interaction that depends on the structural connectivity is irrelevant in the relaxation dynamics of the synchronization in the strong-coupling regime. The relaxation dynamics is analytically derived in a form independent of the system size, and it exhibits good consistency with numerical simulations. As an application, we also explore the recovery dynamics of the oscillators when perturbations enter the system.

DOI: 10.1103/PhysRevE.78.016106 PACS number(s): 89.75.Hc, 05.45.Xt, 89.75.Fb

I. INTRODUCTION

Various oscillatory systems in nature—for example, biological systems such as flashing fireflies, chorusing crickets, cardiac pacemaker cells in the heart, neurons in the brain, and chemical and physical systems such as chemical oscillations and Josephson junction arrays—have been known to exhibit remarkable phenomena of collective synchronization [1–3]. In order to understand such synchronization behaviors, nonlinear coupled oscillators have been extensively studied in diverse branches of science. Among the various oscillator systems, a typical model was proposed and analyzed by Kuramoto [3–5]. The Kuramoto model, where N limit-cycle oscillators are globally (all-to-all) coupled, has been studied extensively due to its analytical tractability. Recently, this model has attracted further attention due to the experimental applications shown in a recent paper [2]. Thus far, the Kuramoto model has been extended with many variations for applications in diverse systems. For example, thermal noise, randomness in the coupling, external force, and time-delayed coupling have been considered in the model, and their effects have been explored [4–7].

Although the all-to-all coupling of the Kuramoto model is analytically tractable and also applicable to some experimental systems, such type of connectivity has a limitation when applied to most real systems. In other words, the interaction (via the connectivity) among the components is neither very regular nor random. Instead, most of the interactions appear to be between these two extreme cases. Accordingly, we need to consider such nontrivial connectivities in the system and extend the study of synchronization to such intermediate network topologies. The dynamics and structural properties of complex networks have recently attracted considerable attention as one of the approaches to understand complex systems in diverse fields [8]. In particular, recent studies on the synchronization of the Kuramoto-type coupled oscillators embedded in complex networks have became representative examples of the study of dynamics on networks. Thus far, Kuramoto synchronies have been extensively studied in terms of the possibility of synchronization transition, its critical behavior, finding of associated critical exponents, and phase diagram along with the stability analysis of the fully synchronized state [9,10]. In *small-world* (SW) networks [11], for example, the synchronization transition occurs at a finite critical coupling strength, even in the case of a very small rewiring probability, and the critical behavior is found to be the same as that of the globally coupled case. Synchronizations have also been studied on *scale-free* (SF) networks [12–15] with the degree distribution given by $P(k)\sim k^{-\gamma}$. However, most of the studies on dynamical systems in complex networks have focused on the stationary properties rather than the dynamics, even though dynamics such as relaxation from the desynchronized state to the synchronized state is very important from the viewpoint of information transfer processes, formation of social consensus, and the response of the system to external perturbations.

In the present paper, we report our study of collective synchronization, with an emphasis on its relaxation dynamics on various complex networks. A globally connected network, SW network, and SF network are considered for the investigation of the relaxation behavior. This paper is organized as follows. In Sec. II, a model system and the method for measuring the relaxation time are explained. In Sec. III, numerical results for each complex network are presented, and Sec. IV presents simulation results for the globally connected network and for the analytic approach. In Secs. V and VI, the collapsing forms of the relaxation and recovery dynamics are presented; finally, Sec. VII summarizes our study.

II. MODEL SYSTEM

The dynamics of N coupled limit-cycle oscillators having the phases $\{\phi_i(t)|i=1,2,\ldots,N\}$ is described by the set of equations

*sonswoo@kaist.ac.kr
†hjeong@kaist.ac.kr
‡hhong@chonbuk.ac.kr

$$\frac{d\phi_i}{dt} = \omega_i - \frac{K}{\langle k \rangle} \sum_{j=1}^{N} a_{ij} \sin(\phi_i - \phi_j). \tag{1}$$

The first term ω_i on the right-hand side of Eq. (1) represents the natural frequency of the ith oscillator, and it is assumed to be randomly distributed according to a normal distribution function that has the correlation $\langle \omega_i \omega_j \rangle = \sigma^2 \delta_{ij}$ with variance σ^2 and zero mean ($\langle \omega_i \rangle = 0$). The second term indicates the coupling between the oscillators; the coupling strength is set to a positive constant ($K > 0$) so that the neighboring oscillators prefer to minimize their phase difference. The adjacency matrix a_{ij} is given by

$$a_{ij} = a_{ji} \equiv \begin{cases} 1, & \text{if } i \text{ and } j \text{ are connected,} \\ 0, & \text{otherwise.} \end{cases} \tag{2}$$

Further, $\langle k \rangle$ denotes the mean degree given by $\Sigma_i k_i / N$, where $k_i = \Sigma_j a_{ij}$. We note that the average degree $\langle k \rangle$ and the coupling strength K affect the evolving time scale, and therefore they may change the relaxation time during the synchronization process. For the case of the globally connected network—for example, $a_{ij} = 1$ for all oscillators excluding self-loops—this value yields $\langle k \rangle = N - 1$, which corresponds to the original Kuramoto model [3]. Previous studies by Kuramoto have shown that there exists a critical coupling strength $K_c = 2/\pi g(0)$ beyond which phase synchronization emerges [3].

Collective phase synchronization is conveniently described by the order parameter defined by

$$r(t) \equiv \left\langle \left| \frac{1}{N} \sum_{j=1}^{N} e^{i\phi_j(t)} \right| \right\rangle, \tag{3}$$

where $\langle \cdots \rangle$ denotes the average over different realizations of intrinsic frequencies as well as networks. We investigate the relaxation of the phase order parameter $r(t)$ above K_c, which describes the synchronization dynamics including the initial transient behavior; we also measure the time required to establish global synchronization [10], which serves as a good indicator for monitoring the information transfer or the system recovery dynamics after a perturbation.

We perform numerical simulations using Eq. (1), where the Gaussian distribution function given by $g(\omega) = (2\pi\sigma^2)^{-1/2} \exp(-\omega^2/2\sigma^2)$ with zero mean and unit variance ($\sigma^2 = 1$) is chosen for convenience. For the numerical integration, we used the Heun method [16] with a time step $\Delta t = 0.01$. In order to avoid a numerical error, we compare our numerical results with those of the fourth-order Runge-Kutta methods with various time steps and we verified that there is no difference under the limit of our simulated network size. The initial phases of the oscillators are randomly chosen from the interval $[0, 2\pi)$, which yields the fully desynchronized phase ($r \approx 0$), and the ordering relaxation from the desynchronized state to the synchronized state ($r \neq 0$) is examined. The phase order parameter $r(t)$ is averaged over 1000 ensembles with different initial phases, natural frequencies, and network realizations at each time. In order to measure the time required for relaxation, we first normalize the order parameter as

$$\tilde{r}(t) \equiv \frac{r(t) - r_{st}}{r_0 - r_{st}} \tag{4}$$

such that $\tilde{r}(0) = 1$ and $\tilde{r}(t \to \infty) = 0$, where $r_0 = r(0)$ and $r_{st} = \lim_{t \to \infty} r(t)$. We then compute the average relaxation time given by [11,17]

$$\tau_r = \int_0^\infty dt' \, \tilde{r}(t'). \tag{5}$$

We note that the average relaxation time τ_r in Eq. (5) is a convenient measure for probing the relaxation dynamics since it is not only robust for obtaining the saturation time, but also useful for a system with many relaxation time scales [17]. However, for some other systems, the order parameter $r(t)$ may not monotonically converge to r_{st}. Therefore, in such cases, the method described in the present paper may not be applicable. For convenience, we use the definitions of both τ_r and τ_{r^2} since τ_{r^2} is easily derived for the mean-field case. We denote the relaxation time of r^2 by τ_{r^2} by using $r^2(t)$ in Eq. (4).

III. RELAXATION ON COMPLEX NETWORKS

We consider complex networks such as SW and SF networks and investigate the relaxation dynamics on these networks by varying their structural properties. The SW and SF networks are constructed following the procedure described in Refs. [18–20]: (i) For the SW networks [18], we first construct a one-dimensional regular network of size N with m-range local connections (we fix $m = 3$ for convenience—i.e., the mean degree $\langle k \rangle = 2m = 6$). Each link is visited once and then removed with the rewiring probability P. Subsequently, it is reconnected to a randomly selected node, thus avoiding self-loops and multiple links. Oscillators are located at each node of the SW network, where a link between two nodes represents the coupling (interaction) between the two oscillators. (ii) The SF networks [19] are generated using the static model [20]. Initially, N nodes are prepared without links. The ith node has the prescribed probability $p_i = i^{-\mu} / \Sigma_j j^{-\mu}$, where μ is given by $1/(\gamma - 1)$ with the expected degree exponent γ of the degree distribution $P(k) \sim k^{-\gamma}$. In order to add a link, we select two nodes i and j having the probabilities p_i and p_j, respectively, and connected them while avoiding self-loops and double links. Such a linking process is repeated until the mean degree $\langle k \rangle$ becomes equal to 6.

We perform numerical integrations of Eq. (1) for the SW and SF networks. The temporal evolution of the phase order parameter $r(t)$ is shown in Figs. 1(a) and 1(c). It is found that the relaxation time required for the oscillators on the SW network logarithmically increases with the system size ($\tau_{r^2} \sim \ln N$) [see Fig. 1(b)]. A smaller rewiring probability P is found to yield slower relaxation dynamics. Similarly, the relaxation dynamics of the SF network also exhibits a logarithmic increasing behavior with an increase in the system size. Furthermore, the relaxation behavior is found to strongly depend on the heterogeneity of the SF network that is characterized by the degree exponent γ [see Fig. 1(d)] in such a

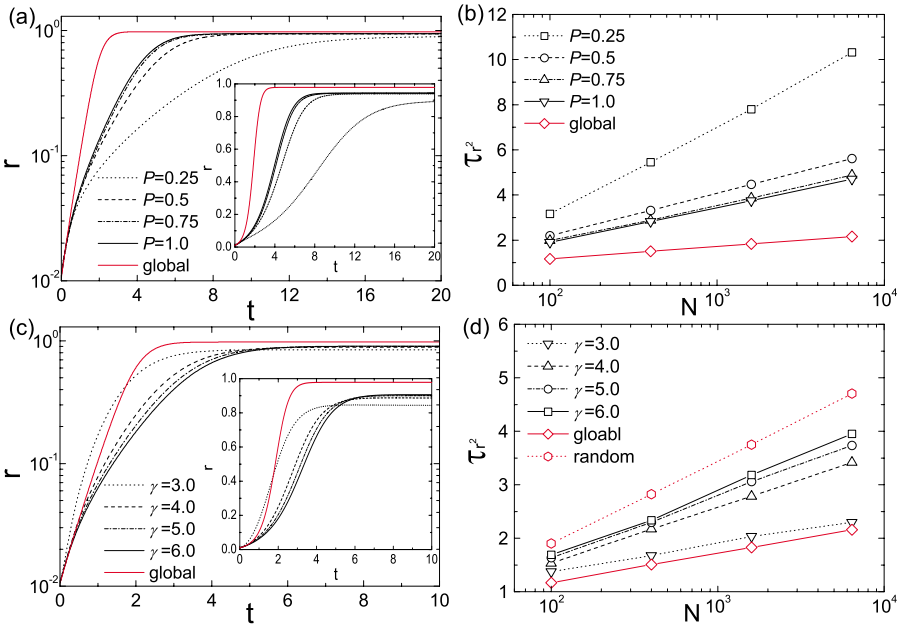

FIG. 1. (Color online) Temporal evolution of the phase order parameter $r(t)$ for (a) SW network and (c) SF network for $K=5$ and $N=6400$ on a semilogarithmic scale. Inset: the y axis is set as a linear scale. The average relaxation time is shown by varying the rewiring probability P and the degree exponent γ for (b) SW networks and (d) SF networks, respectively. The logarithmic dependence ($\tau_{r^2} \sim \ln N$) is clearly shown. The data for the case of a globally coupled network are also shown as a reference (see the text).

manner that a less heterogeneous network exhibits slower dynamic behavior. In order to further study the origin of the logarithmic relaxation time, we reexamine the original Kuramoto model in the next section.

IV. RELAXATION ON ALL-TO-ALL CONNECTED NETWORK

We consider the globally coupled oscillators of the Kuramoto model. Figure 2 shows the time evolution of the order parameter $r(t)$ for the globally connected network in the strong-coupling regime ($K=5>K_c$) [21]. For small t, it is found that the phase order parameter $r(t)$ shows an exponential growth that is well described by $r(t) \sim r_0 \exp(\lambda t)$, with $\lambda \approx 2.143$ and system-size-dependent constant r_0. A larger system is found to attain global synchronization more slowly. In Fig. 3, the relaxation time τ_r is plotted as a function of the network size N for various values of coupling strength K. We also find that the relaxation time τ_r increases logarithmically with the network size ($\tau_r \sim \ln N$).

To understand such logarithmic dependence, we investigate the transient behavior of the order parameter $r(t)$, which has been analytically studied for the globally coupled oscillator system. It is found that the time evolution of $r(t)$ is given by $r(t) \sim r_0 \exp(\lambda t)$, where λ is determined by the relation [22]

$$1 = \sqrt{\frac{\pi}{8}} \frac{K}{\sigma} \exp\left(\frac{\lambda^2}{2\sigma^2}\right) \mathrm{erfc}\left(\frac{\lambda}{\sqrt{2}\sigma}\right) \tag{6}$$

by using the complementary error function $\mathrm{erfc}(x)$. For coupling strength $K=5$ and unit variance ($\sigma^2=1$), Eq. (6) yields $\lambda=2.143$, which corresponds to a slope of 0.931 in the y axis of the base-10 logarithm, exhibiting a good agreement with the slope shown in Fig. 2. The relaxation dynamics of this particular order parameter is given by $dr/dt=\lambda r+br^3+\mathcal{O}(r^5)$ for the case of a symmetric distribution of the intrinsic frequency, where b is a coefficient with a negative value in the supercritical regime ($K>K_c$) [23]. We follow the relaxation dynamics derived by Crawford [23], retaining the terms up to $\mathcal{O}(r^3)$. Further, the coefficient b is obtained so as to match the experimental observation. In a long-time limit, $r(t)$ attains the steady state r_{st}. The coefficient b is then determined to be $-\lambda/r_{st}^2$, and the equation of motion for $r(t)$ is written as

$$\frac{dr(t)}{dt} = \lambda r\left(1 - \frac{r^2}{r_{st}^2}\right), \tag{7}$$

which yields

$$r^2(t) = \frac{r_{st}^2 r_0^2 \exp(2\lambda t)}{r_{st}^2 - r_0^2 + r_0^2 \exp(2\lambda t)}. \tag{8}$$

For small t, $r^2(t)$ in Eq. (8) is approximated as $r^2(t) \simeq r_0^2 \exp(2\lambda t)$, which is Strogatz and Mirollo's result [22]. The relaxation time is then easily found to be proportional to $\ln N$:

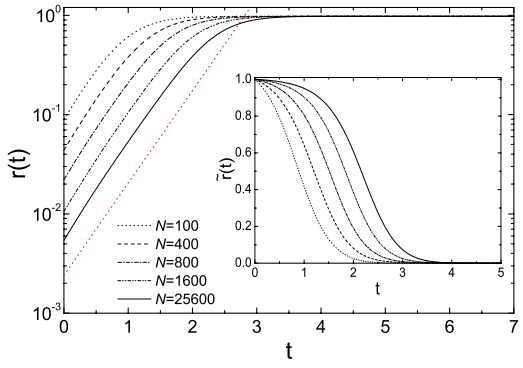

FIG. 2. (Color online) Phase order parameter $r(t)$ is plotted as a function of time t for globally coupled networks for $K=5$ by varying the network size N. The red dotted line is a guide for the eye with a slope of 0.931. Inset: the evolution of the normalized order parameter $\tilde{r}(t)$ vs time t.

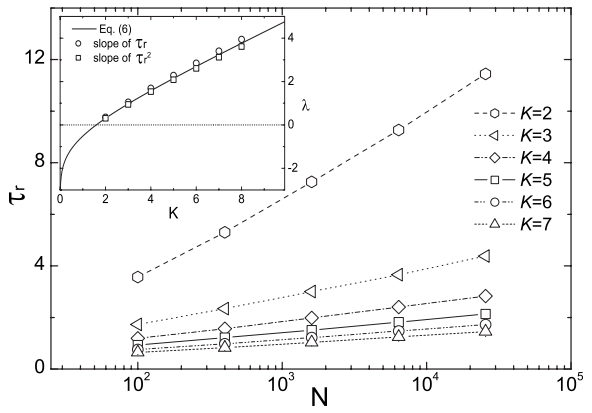

FIG. 3. Averaged relaxation time τ_r is plotted as a function of the system size N for various coupling strengths K (on the semilogarithmic scale) for the system of globally coupled oscillators, displaying a logarithmic increase with the network size ($\tau_r \sim \ln N$). Inset: the slope measured in the plot of τ_r (τ_{r^2}) vs K is shown, and the solid line represents the theoretical prediction given by Eq. (6).

$$\tau_{r^2} = \frac{1}{2\lambda}\frac{r_{st}^2}{r_{st}^2 - r_0^2}[\ln r_{st}^2 - \ln r_0^2] \simeq \frac{1}{2\lambda}\ln N + \tau_0, \tag{9}$$

where τ_0 is a constant independent of the network size N. One can also observe that $r^2(t)$ is a sigmoid function and Eq. (8) is equivalent to

$$\frac{r^2(t)}{r_{st}^2} = \frac{1}{1+\exp[-2\lambda(t-t_c)]}, \tag{10}$$

with t_c, where t_c is a single constant, $r^2(t_c) = r_{st}^2/2$, and $\tau_{r^2} \simeq t_c$ for large N since the sigmoid function has a point symmetry and the integral of Eq. (5) becomes t_c.

As expected, the initial phase order parameter is given by $r_0 \sim \mathcal{O}(N^{-1/2})$ since the N initial phases of the oscillators are randomly scattered. On the other hand, r_{st} is size independent for large N, and it saturates near 1, as shown in Eq. (9). Therefore, it is evident that the origin of the logarithmic increase in the relaxation time lies in the initial random phases. In order to confirm this, we first investigate the possibility of the collapsing of all the data when they are shifted by an amount equal to the relaxation time along the time axis. It is observed that the data correspond to a curve that strongly supports our prediction (see Fig. 4). We also verify the collapse of all lines into a single sigmoid function, which is represented by Eq. (8), with the exception of the overshooting that occurs near the saturation time due to the neglected $\mathcal{O}(r^5)$ terms. Second, we examine how the result is changed when networks with different sizes begin at the same value of r_0. In order to set the same value of r_0 for different system size N, we removed the N dependence of the initial value of the order parameter r_0 in following manner. We generate $N=100$ random numbers for the initial phase $\phi_i(0)$. In order to assign 200 random phases to N, we first generate 100 random numbers and then use them twice. In other words, we select only 100 random numbers and reuse them $N/100$ times. In this manner, we simply suppress the initial fluctuation in r_0, maintaining a constant value that is

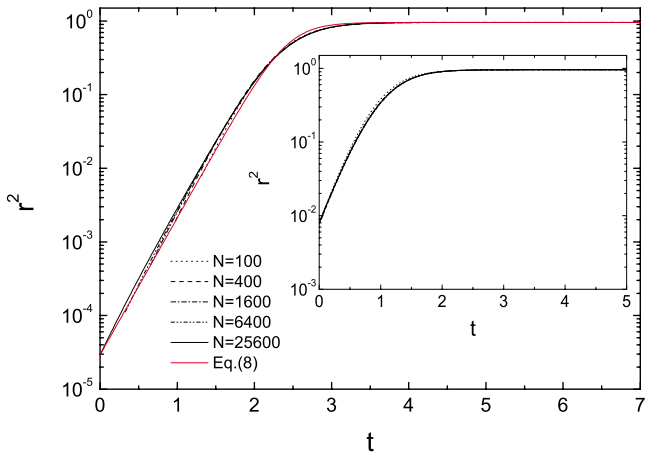

FIG. 4. (Color online) Time-shifted $r^2(t)$ is plotted as a function of time t. Each curve of Fig. 2 is shifted along the x axis as the difference of the relaxation time from that of $N=25\,600$. The red line corresponds to Eq. (8). All data points lie along a single curve. Inset: for different networks sizes, $r(t)$ starts from the same initial value r_0 by restricting the number of possible initial phases in which all the data points collapse along a curve.

independent of the system size N. The suppression of the fluctuation in the initial phases is found to result in the disappearance of the logarithmic dependence for the relaxation time. This is also numerically confirmed (see the inset of Fig. 4). These two results support the fact that the logarithmic behavior of the relaxation time is actually attributed to the fluctuation in the initial phases.

V. COLLAPSING OF THE RELAXATION DYNAMICS

On the assumption that the topological differences in networks do not significantly alter the evolution of the synchronization order parameter, but alter the speed at which global synchronization is attained, we investigate the collapsing of the relaxation dynamics given by Eq. (10) for various complex networks. We examine the data collapse by varying the control parameters a and t_c in $r^2(t) = r_{st}^2/\{1+\exp[-2\lambda(t-t_c)/a]\}$, where a tunes the synchronization speed by dividing the exponential growth rate λ and t_c corresponds to the relaxation time for each complex network. As shown in Fig. 5, all the data points for various complex networks with different system sizes from $N=100$ to $N=25\,600$ are found to exhibit a good collapse on a single sigmoid function. The scaling constants a and t_c are measured for various values of the rewiring probability P and degree exponent γ. Figure 6 shows the control parameters a and t_c as a function of P and γ. When the rewiring probability P of the SW networks decreases, t_c and a rapidly increase near $P=0$ [see Fig. 6(a)] and become saturated for large-P regimes. For the SF networks, this rapidly increasing behavior is observed from the region of small γ to large γ, but it is eventually saturated in the large-γ regime [see Fig. 6(b)]; this is similar to the case of SW networks. It is interesting to note that the oscillators on the SW and SF networks are influenced only by the nearest neighbors via local interactions; however, the relaxation behavior is similar to that of globally connected networks.

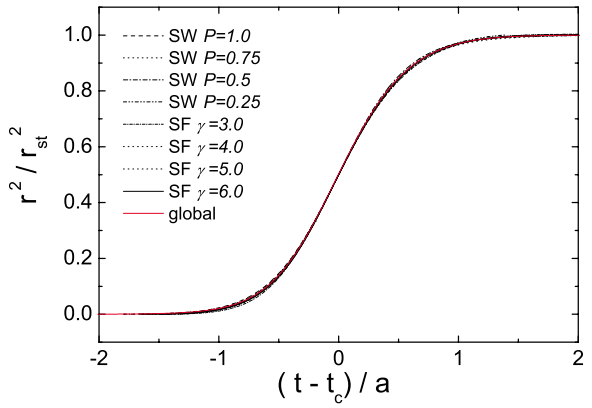

FIG. 5. (Color online) Collapse of the data $r^2(t)/r_{st}^2$ for different network sizes of SW and SF networks is shown, displaying a good coincidence in one sigmoid function with the control parameter a and t_c. The red line is an amplitude evolution line of the globally connected network, and it is provided as a reference.

When the coupling strength K approaches to $K_c+\Delta$ ($\Delta>0$), the relaxation time increases; however, our result remains valid, as shown in Fig. 3. At the region very close to K_c, on the other hand, the size of the synchronized cluster becomes unstable and the order parameter value is very small; furthermore, the fluctuation by the desynchronized oscillators becomes relevant. Therefore, the validity of our result in the regime very close to K_c is not obvious. Further, the relaxation dynamics at the critical point K_c is found to show a totally different behavior, exhibiting a power-law decay instead of an exponential one [24].

VI. RECOVERY FROM A PERTURBATION

In this section, we consider the recovery dynamics of the oscillators when a perturbation enters the system. From a

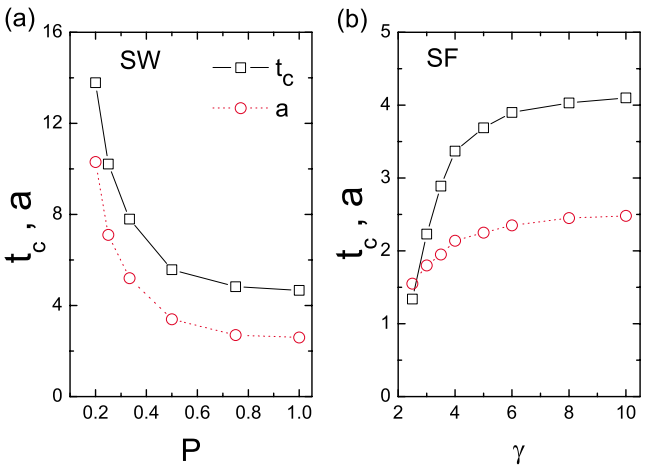

FIG. 6. (Color online) Relaxation time t_c and control parameter a for (a) SW network and (b) SF network for $K=5$ and $N=6400$. The control parameter a is independent of the network size N and only depends on the network topology and coupling strength K. The control parameter t_c is linearly proportional to the relaxation time τ_{r^2}. Therefore, t_c also shows a logarithmic increasing tendency with the network size.

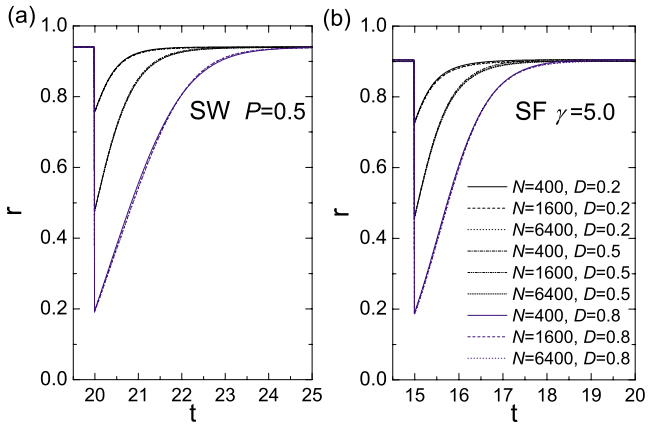

FIG. 7. (Color online) Response of the system to a perturbation is plotted for various network sizes. From the steady state, each oscillator is reset to the random phase with a damage probability D for (a) SW networks and (b) SF networks. The legend of (a) is identical to that of (b).

different viewpoint, oscillators with completely random phases could be considered to lose the entire phase information of the synchronized system; i.e., 100% damage is done to the system. Since the system is in the strong-coupling regime, it will eventually return to the synchronized state. However, if a synchronized system sustains partial damage, it is of interest to know how fast the system recovers its normal state. We have probed the network size dependence of the recovery time under a partial perturbation. The oscillators are launched from a random initial condition with a strong-coupling strength $K>K_c$. After the system attains the steady state, oscillators that are randomly selected with a probability D will be perturbed. In other words, each oscillator loses its phase information with a damage probability D and is assigned a random phase. We then observe the dynamics during the recovery to the synchronized state for different network sizes and different damage probabilities D for 1000 ensembles. The results are shown in Fig. 7; the recovery dynamics after perturbation is also independent of the network size N since the initial condition r_0 is identical for the same value of D when D is sufficiently small, which is consistent with the result of the previous sections. When the damage approaches 1, the logarithmic size dependence appears, as shown in Fig. 8. This is because even the effect of the fluctuation given by $\mathcal{O}(N^{-1/2})$ is small as compared to $r_0\approx 1$ in the small-D regime. On the other hand, the effect of fluctuations in the large-D regime increases as compared to $r_0\approx 0$. It is found that the recovery time is independent of the system size when the damage is small, but depends on the dimensions of the damaged part.

In addition, to sustaining damage to the SF networks, we consider two different methods according to the degree preference. It is well known that a node with a large degree (hub) causes greater damage to the integrity and characteristic path length (CPL) of the network [25]. Since the importance of each node in the SF networks is different depending on its degree, the tendency of synchronization can also be changed by using the degree of the damaged node. The phase information of each node is erased beginning from the node with

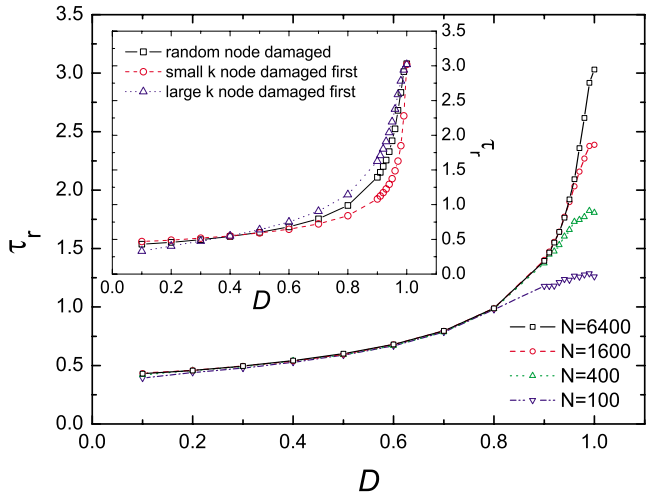

FIG. 8. (Color online) Relaxation time τ_r under damage D for different sizes of SF networks (γ=5). The network size dependence of the relaxation time appears only in the regime of large damage D near 1. Inset: relaxation time dependence for different types of node damages (N=6400). When large (small) degree nodes are damaged first, the system recovers faster (slower) than random damaging at the small-D regime; however, at the large-D regime, it is vice versa.

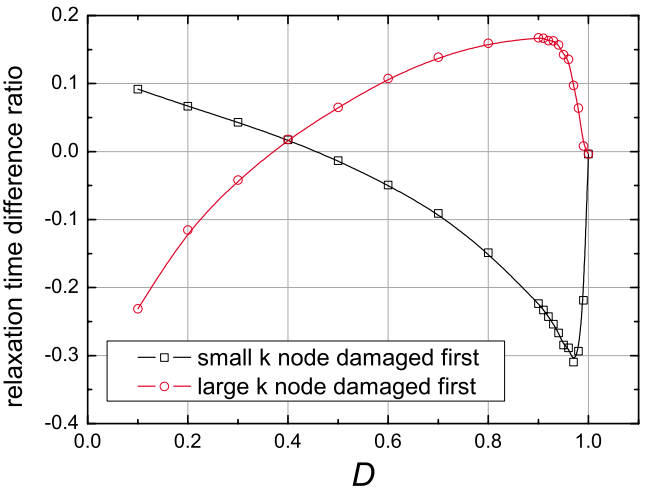

FIG. 9. (Color online) Ratio of the relaxation time difference for the degree preferential method to that for the random damaging method.

the smallest (largest) degree in increasing (decreasing) order until $\lfloor DN \rfloor$ nodes are damaged. These two different methods apparently alter the speed of recovery (relaxation time), but the relaxation time remains almost independent of the system size. It is interesting to note that when damages are first sustained by a node with a large degree, the system recovers the normal state earlier than in the case of random node damage for small D values. However, at large D values, the degree preference damage induces heavier shocks in the system as compared to those by a random damage (see the inset of Fig. 8). The ratio of the relaxation time difference of each degree preferential damaging method to that of the random damaging method shows this behavior more clearly (see Fig. 9). The positive (negative) value implies slower (faster) recovery as compared to random damaging. When the hub nodes are damaged first, contrary to our expectation, the system recovers faster than in any other case, which is similar to the result in the Ref. [12], where the authors change the phase of a node by π after the synchronization process attains the steady state and measure the average time required for a node to again be in the synchronized cluster as a function of its degree. Even in the extreme case $D=1/N$ of our simulation, the result can be explained by the same argument. This is because when the hubs are damaged, their neighbors provide the same phase information and the random phase of the hub is absorbed by many neighbors in a manner similar to a buffer. Moreover, the hub node rapidly shifts to the steady phase since hubs have more connections than average, which implies that the effective coupling strength of a hub is larger than the average value. However, when a large damage D is first introduced in the system through a large-k node, the population of undamaged neighbor nodes is not sufficient to recover the system. In such cases of severe damage, the survival of the large-degree nodes is advantageous. Therefore, in the large-D regime, the system in which a node with a small degree is first damaged recovers more quickly.

VII. SUMMARY AND DISCUSSION

In summary, we investigated the relaxation dynamics of synchronization in a large number of coupled oscillators on various complex networks. We considered SW and SF networks as well as all-to-all connected networks (complete graph) and explored the relaxation behavior of the phase order parameter $r(t)$ from the desynchronized state to the synchronized state. Following Crawford's analysis, we derived the evolution equation of $r^2(t)$ in a globally coupled network; the results obtained from this equation showed good consistency with the numerical simulation results. We find that the relaxation time for the globally connected network increases logarithmically with network size. Moreover, for the SW and SF networks, it is observed that the relaxation times exhibit similar logarithmic behaviors. We find that such a logarithmic increase is attributed to the contribution from the randomness of the initial phases. The collapsing form of the relaxation dynamics is also derived, and it exhibits good agreement with the numerical simulations. As an application, we explore the recovery dynamics of the oscillators when perturbations enter the system.

It is of interest to know whether the logarithmic increase in the relaxation time on complex networks can be attributed to the increase in the CPL or the diameter of the networks because they exhibit a similar logarithmic increase ($\ell \sim \ln N$). While traversing the path to synchronization, each oscillator attempts to minimize the phase difference relative to its neighbors' phase. This minimizing process can be interpreted as the oscillators interchanging phase information among themselves through the networks. Therefore, one may consider that the relaxation time depends on the CPL or the diameter of the network through which information initiated from an oscillator spreads to all the oscillators. In order to verify this, we measure the CPL for various degree expo-

nents and investigate the correlation between these two quantities. However, interestingly, we observe that the logarithmic increase in the relaxation time results from the randomness of the initial phase and not from the logarithmically increasing behavior of the CPL. If we consider the all-to-all connected network, it is more obvious since the CPL of the globally connected network is exactly equal to 1 ($\ell=1$), independent of the network size N. Therefore, the logarithmic dependence does not originate from the system-size-dependent CPL.

It is very important to know how synchronization emerges globally and also examine how local nucleation occurs. Unfortunately, in this study, we did not follow the local events since we have used the global order parameter. Recent papers suggest a method for observing how the local patterns of synchronization emerge [26]. It is necessary to combine the global and microscopic aspects involved in attaining synchronization since this would be valuable as a future study.

While preparing this paper, we learned of a study by Almendral and Díaz-Guilera [27], which partly overlaps with ours. They show that the synchronization time depends on the smallest nonzero eigenvalue of the Laplacian matrix in the complete synchronization problem. Interestingly, the synchronization time dependence relation is basically similar to our derivation, Eq. (5). However, in our study, we focus on the dependence of the synchronization time on the network topology and system size N for the Kuramoto model of the partial synchronization problem with a more general Gaussian distribution of natural frequencies. It is of great interest that the argument about the synchronization time dependence on network topology can be extended to general synchronization problems.

ACKNOWLEDGMENTS

We thank Pan-Jun Kim and Beom Jun Kim for their useful discussions. This work was supported by Korea Research Foundation Grant No. KRF-2006-312-C00548 (H.J.) and by KOSEF via Grants No. R01-2007-000-20084-0 (H.H.) and No. R17-2007-073-01001-0 (S.S.).

[1] A. T. Winfree, *The Geometry of Biological Time* (Springer-Verlag, New York, 1980); A. S. Pikovsky, M. G. Rosenblum, and J. Kurths, *Synchronization: A Universal Concept in Nonlinear Sciences* (Cambridge University Press, Cambridge, England, 2001).

[2] I. Z. Kiss, Y. M. Zhai, and J. L. Hudson, Science **296**, 1676 (2002); Phys. Rev. Lett. **94**, 248301 (2005).

[3] Y. Kuramoto, in *Proceedings of the International Symposium on Mathematical Problems in Theoretical Physics*, Lecture Notes in Physics, edited by H. Araki (Springer-Verlag, New York, 1975); Y. Kuramoto, *Chemical Oscillations, Waves, and Turbulence* (Springer-Verlag, Berlin, 1984); Y. Kuramoto and I. Nishikawa, J. Stat. Phys. **49**, 569 (1987).

[4] J. A. Acebrón, L. L. Bonilla, C. J. Pérez Vicente, F. Ritort, and R. Spigler, Rev. Mod. Phys. **77**, 137 (2005).

[5] H. Daido, Prog. Theor. Phys. **77**, 622 (1987); Phys. Rev. Lett. **68**, 1073 (1992).

[6] L. L. Bonilla, C. J. Pérez Vicente, and R. Spigler, Physica D **113**, 79 (1998).

[7] H. Sakaguchi and Y. Kuramoto, Prog. Theor. Phys. **76**, 576 (1986); H. Sakaguchi, *ibid.* **79**, 39 (1988); M. K. Stephen Yeung and S. H. Strogatz, Phys. Rev. Lett. **82**, 648 (1999).

[8] S. H. Strogatz, Nature (London) **410**, 268 (2001).

[9] L. M. Pecora and T. L. Carroll, Phys. Rev. Lett. **80**, 2109 (1998); M. Barahona and L. M. Pecora, *ibid.* **89**, 054101 (2002); T. Nishikawa, A. E. Motter, Y. C. Lai, and F. C. Hoppensteadt, *ibid.* **91**, 014101 (2003); H. Hong, B. J. Kim, M. Y. Choi, and H. Park, Phys. Rev. E **69**, 067105 (2004).

[10] The *fully synchronized state* here means the state where all the phases of oscillators are same ($\phi_1=\phi_2=\cdots=\phi_N$), yielding the order parameter $r=1$. On the other hand, when the order parameter shows a nonzero value, but smaller than 1 ($0<r<1$), we call the state as the *partially synchronized state*. We also call it *global synchronization*, where it implies the emergence of a macroscopic cluster of synchronized oscillators with a system size of $\mathcal{O}(\mathcal{N})$.

[11] H. Hong, M. Y. Choi, and B. J. Kim, Phys. Rev. E **65**, 026139 (2002).

[12] Y. Moreno and A. F. Pacheco, Europhys. Lett. **68**, 603 (2004).

[13] T. Ichinomiya, Phys. Rev. E **70**, 026116 (2004).

[14] J. G. Restrepo, E. Ott, and B. R. Hunt, Phys. Rev. E **71**, 036151 (2005).

[15] D.-S. Lee, Phys. Rev. E **72**, 026208 (2005); E. Oh, D.-S. Lee, B. Kahng, and D. Kim, *ibid.* **75**, 011104 (2007).

[16] R. L. Burden and J. D. Faires, *Numerical Analysis* (Brooks-Cole, Pacific Grove, CA, 1997).

[17] B. J. Kim, M. Y. Choi, S. Ryu, and D. Stroud, Phys. Rev. B **56**, 6007 (1997).

[18] D. J. Watts and S. H. Strogatz, Nature (London) **393**, 440 (1998).

[19] R. Albert and A.-L. Barabási, Rev. Mod. Phys. **74**, 47 (2002); S. N. Dorogovtsev and J. F. F. Mendes, Adv. Phys. **51**, 1079 (2002); M. E. J. Newman, SIAM Rev. **45**, 167 (2003).

[20] K.-I. Goh, B. Kahng, and D. Kim, Phys. Rev. Lett. **87**, 278701 (2001).

[21] The critical coupling strength for the Kuramoto model is known to be $K_c=2/\pi g(0)$ [3], which corresponds to $K_c\approx 1.6$ for the case of unit variance.

[22] S. H. Strogatz and R. E. Mirollo, J. Stat. Phys. **63**, 613 (1991).

[23] J. D. Crawford, J. Stat. Phys. **74**, 1047 (1994); Phys. Rev. Lett. **74**, 4341 (1995); S. H. Strogatz, Physica D **143**, 1 (2000).

[24] The detailed critical behavior at the critical point K_c is planned to be published elsewhere.

[25] R. Albert, H. Jeong, and A.-L. Barabási, Nature (London) **401**, 130 (1999).

[26] J. Gomez-Gardenes, Y. Moreno, and A. Arenas, Phys. Rev. Lett. **98**, 034101 (2007); Phys. Rev. E **75**, 066106 (2007).

[27] J. A. Almendral and A. Díaz-Guilera, New J. Phys. **9**, 187 (2007).